Eur Phys J C **34**, s01, s39–s48 (2004)
Digital Object Identifier (DOI) 10.1140/epjcd/s2004-04-005-y

EPJ C direct
electronic only

The startup of Run II: Status of Tevatron, CDF, and DØ

Jianming Qian, for the CDF and DØ Collaborations

Department of Physics, University of Michigan, Ann Arbor, Michigan 48109, e-mail: qianj@umich.edu

Received: 1 October 2003 / Accepted: 17 November 2003 /
Published Online: 13 July 2004 – © Springer-Verlag / Società Italiana di Fisica 2004

Abstract. I briefly summarize the current status of Tevatron Run II, and highlight a few preliminary results from the CDF and DØ experiments.

PACS. 1 3.85.Lg – 14.54.Ha – 14.70.-e – 14.80.-j

1 The Tevatron collider

Since the conclusion of the previous data-taking period in 1996 (Run I), the Tevatron complex has undergone extensive upgrade [1]. New in Run II are a) a main injector storage ring for 150 GeV proton replacing the old main ring; b) 36 colliding bunches instead of 6 resulting in a shorter 396 ns bunching crossing time; c) an increased center-of-mass energy from 1.8 TeV to 1.96 TeV; d) a new storage ring of permanent magnets (called recycler) for accumulating anti-protons. The first phase (Run IIa) of the upgrade, implementing items a)-c), is designed to deliver a peak luminosity of 8×10^{31} cm^{-2} s^{-1} and an integrated luminosity of 2 fb^{-1}. The second phase (Run IIb), with the recycler, is advertised to deliver $3-4 \times 10^{32}$ cm^{-2}s^{-2} peak and 10+ fb^{-1} integrated luminosity per experiment before the Large Hadron Collider (LHC) at CERN turns on. Options of even shorter 132 ns bunching crossing and antiproton recycling to the recycler from the Tevatron at the end of a store were considered for Run IIb, but were subsequently dropped due to schedule and technical risks and limited expected return. A schematic of the Tevatron complex is shown in Fig. 1.

The startup of Run II has proven to be more challenging than most of us had imagined. More than two years since the official start of Run II, the Tevatron has yet to reach its design Run IIa luminosity, both instantaneous and integrated. Although the peak luminosity achieved so far is still low, a more serious problem appears to be its reproducibility. As shown in Fig. 2, the weekly delivered luminosity has fluctuations from week to week. As of September 7, 2003 (the beginning of the 2003 shutdown), a total of ∼340 pb^{-1} has been delivered. Of this total, 239 pb^{-1} was delivered in fiscal year 2003 (October 2002 to September 2003), meeting the 'revised' goal of 225 pb^{-1} for the past year. A history of peak store luminosity is shown in Fig. 3. The highest peak luminosity achieved so far is about 4.9×10^{31} cm^{-2} s^{-1}, compared the design of 8×10^{31} cm^{x-2} s^{-1}.

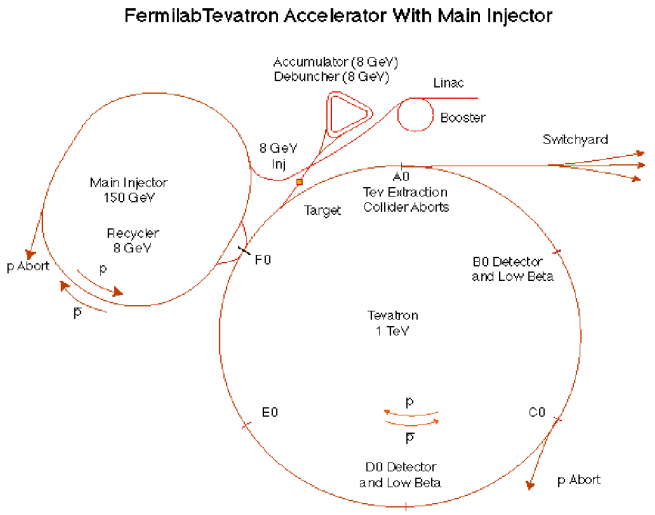

Fig. 1. Schematic of the Tevatron complex

There is no single magic bullet to solve the luminosity problem. A number of projects on the accumulator, beam line, longitudinal dampers of the main injector, etc, are being worked on with each expected to provide an improvement of 5-15%. The hope is that the combination of these will lead to the designed peak luminosity, and this, together with more reliable operation, will soon deliver the integrated luminosity of Run IIa. For the longer-term, the major limitation to the luminosity is the antiproton production rate, currently a factor of five below what is needed to achieve the design luminosity of Run IIb. Potential improvements involve a factor of two from protons on target, a factor of 2-2.5 from an increase in antiproton acceptance, and a factor of 2 from many small incremental improvements.

There are many technical and schedule risks to this plan. The Laboratory has recently revised its long-term plan [2] submitted to the US Department of Energy, the

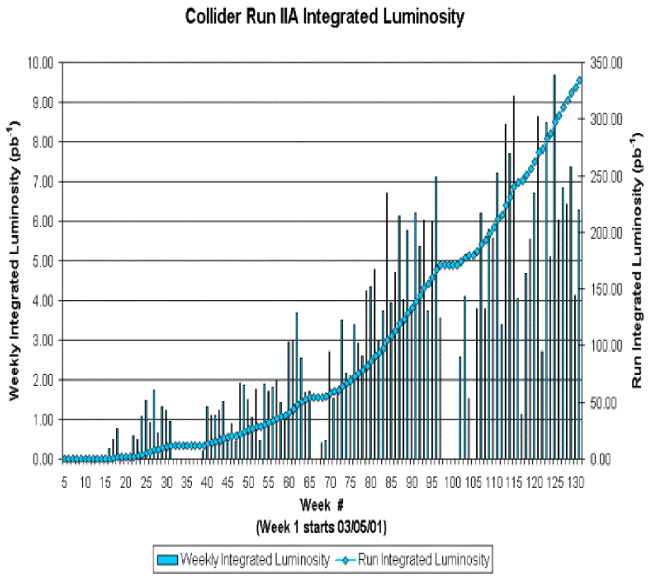

Fig. 2. Weekly and integrated luminosity delivered by the Tevatron from March 05, 2001 up to September 7, 2003, the beginning of the 2003 shutdown

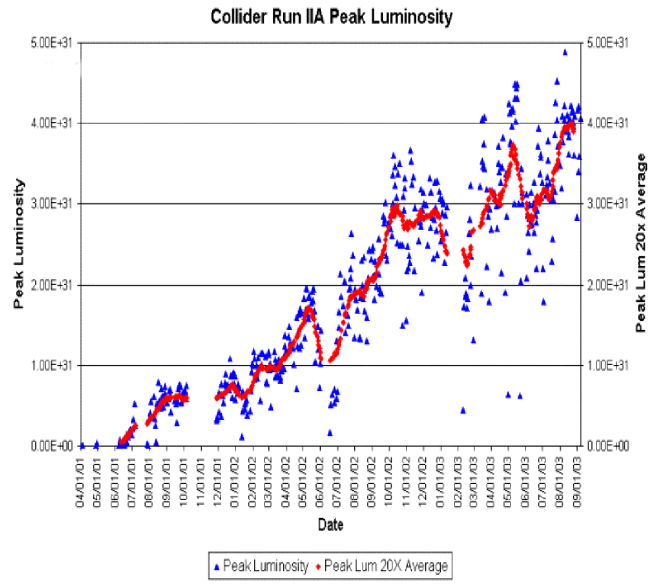

Fig. 3. Peak store luminosity and 20-store moving average

funding agency of the Laboratory. The luminosity profile for the new plan is shown in Fig. 4, and it projects a lower luminosity than before. The conservative (or 'base') plan projects an integrated luminosity of 4.4 fb^{-1} through October 2009 while the more aggressive plan (or 'stretched') projects a total of 8.6 fb^{-1} over the same period. The stretched plan assumes that all planned accelerator upgrades will achieve ∼80% of its technical limit. Electron cooling in the recycler, needed by October 2004, represents a significant challenge to the stretched plan. The new projection is significantly lower than what was planned a couple of years ago. Based on the revised profile, the upgrade of the CDF and DØ silicon detectors was called into question. The silicon detectors, key to much of the physics, are expected to degrade their performance gradually from radiation damage and natural attrition. Although estimates vary, it is generally believed that new silicon detectors will be needed after an integrated luminosity of 3-4 fb^{-1}. On September 2, 2003, the Fermilab director informed the two collider experiments of his decision [3] to discontinue the Run IIb silicon upgrade, but to continue his commitment to Run II.

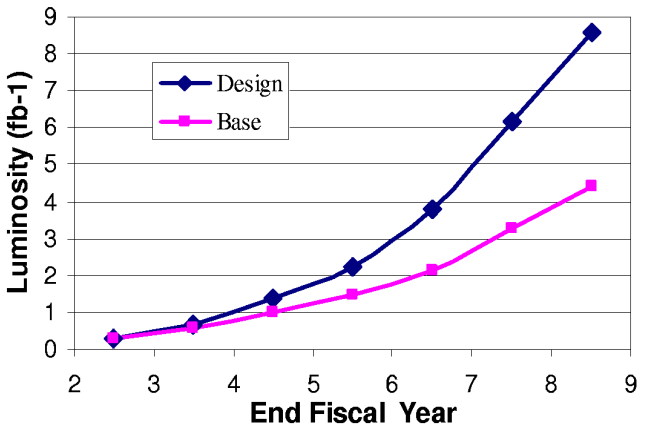

Fig. 4. The revised luminosity profile (fiscal year runs from October to September)

2 The CDF and DØ detectors

To fully exploit the physics potential of the improved Tevatron Collider, both CDF [4] and DØ [5] detectors went through extensive upgrades for Run IIa. For CDF, retained from Run I are a 1.4 Tesla solenoid, central calorimeter and muon detector. The upgrade includes a new tracking system, an end-plug calorimeter, intermediate muon detectors, time-of-flight system, front-end electronics as well as trigger and data acquisition system. The tracking system consists of a silicon vertex detector, intermediate silicon layers, and a central outer tracker. A quadrant of the CDF detector is illustrated in Fig. 5. The CDF detector is operating well. In early May 2003, CDF reported to have about 160 pb^{-1} of data on tape.

Like the CDF detector, the DØ detector also went through an extensive upgrade. Only three major systems from Run I were kept. They are the liquid argon calorimeter, the central muon detector and muon toroid. The entire Run I non-magnetic inner tracking system has been replaced by a magnetic tracker comprised of a five-barrel silicon micro-vertex detector, a state-of-the-art scintillating fiber detector, a 2 Tesla superconducting magnet, and central and forward preshower detectors. In addition, the trigger and data acquisition systems have been upgraded to meet the challenges posed by the improved Tevatron Collider. Figure 6 shows the major components of the DØ detector in Run II. DØ reported about 110 pb^{-1} recorded luminosity at this symposium.

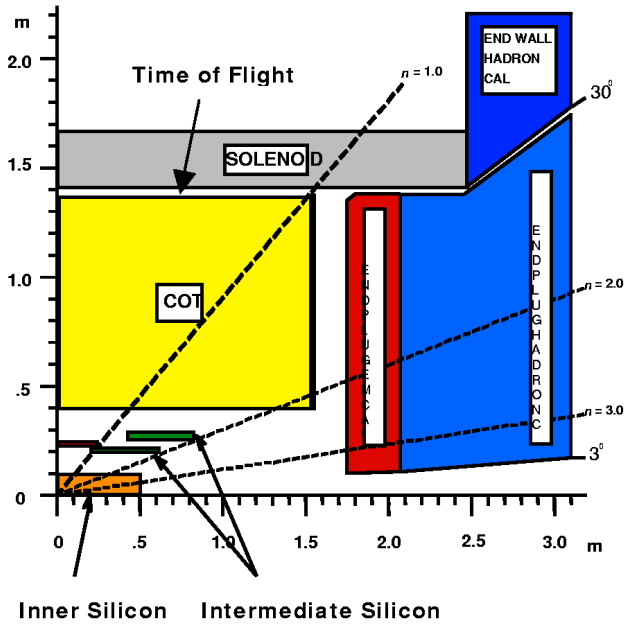

Fig. 5. A schematic view of a quadrant of the upgraded CDF detector

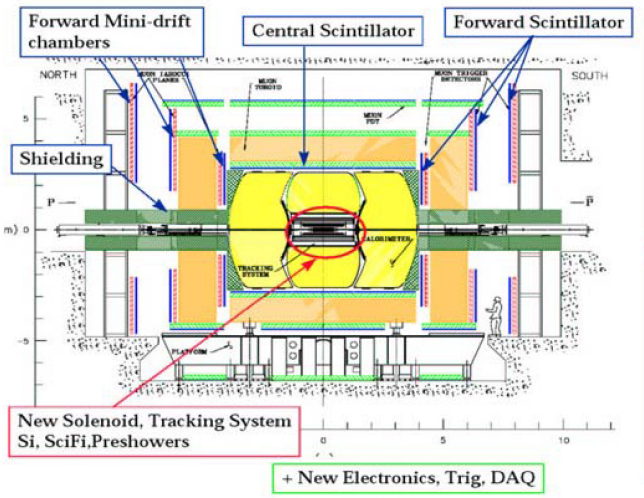

Fig. 6. Side view of the upgraded DØ detector, indicating the major new components

3 Physics

Both CDF and DØ have produced impressive preliminary results from their initial data. These results were obtained from data samples varying from 40 to over 100 pb^{-1}. Many new and improved results have been presented recently at the Lepton-Photon conference held at Fermilab. However, for the record, only those results presented at this symposium will be highlighted in this report. Furthermore, I apologize for not being able to summarize all the results or discuss any results in details. Fortunately, there are other presentations from CDF and DØ at this symposium, and interested readers are suggested to consult these contributions [6,7] in this proceeding.

3.1 Electroweak physics

W and Z bosons are produced copiously at the Tevatron. The simple topology, easy trigger and identification, high rate and small background for their decays to electrons and muons make these final states ideal for calibration and precision measurements. In a way, W and Z decays to leptons (electrons and muons) are the standard candles of high p_T physics at hadron colliders. A $W \to e\nu$ candidate from CDF is shown in Fig. 7(a). $W \to e\nu$ events are selected by requiring a high p_T electron and large missing transverse momentum. As shown in Fig. 7(b), a requirement on large transverse momentum imbalance rejects most of multijet background (due to misidentification of jets as electrons and mismeasurements of transverse momentum imbalance). Similarly, $Z \to ee$ events are easily selected by requiring two high p_T electrons. Typical selection efficiency is ∼20% for $W \to ev$ events and ∼10% for $Z \to ee$ events. CDF selected 38,625 $W \to ev$ and 1,830 $Z \to ee$ candidates from a sample of about 72 pb^{-1}. The estimated backgrounds are about 6% and 0.6% for the two samples. From these events, CDF determined the W and Z production cross sections multiplied by their decay branching ratios to electrons to be:

$$\begin{aligned}\sigma_W \bullet B(W \to ev) &= 2.61 \pm 0.01(\text{stat}) \pm 0.09(\text{sys}) \\ &\quad \pm 0.16(\text{lum})\ \text{nb} \\ \sigma_Z \bullet B(Z \to ee) &= 0.267 \pm 0.006(\text{stat}) \pm 0.012(\text{sys}) \\ &\quad \pm 0.015(\text{lum})\ \text{nb}\end{aligned}$$

where the first error is statistical, the second systematic, and the third is due to the 6% uncertainty on the luminosity. These measurements are to be compared with the NNLO calculations [8] at $\sqrt{s} = 1.96$ TeV:

$$\begin{aligned}\sigma_W \bullet B(W \to ev) &= 2.69 \pm 0.10\text{nb} \\ \text{and } \sigma_z \bullet B(Z \to ee) &= 0.252 \pm 0.009\ \text{nb}\end{aligned}$$

DØ selected 27,370 $W \to ev$ and 1,139 $Z \to ee$ candidates from a recorded data sample of 42 pb^{-1} which led to the measurements:

$$\begin{aligned}\sigma_W \bullet B(W \to ev) &= 3.054 \pm 0.100(\text{stat}) \pm 0.086(\text{sys}) \\ &\quad \pm 0.305(\text{lum})\ \text{nb} \\ \sigma_Z \bullet B(Z \to ee) &= 0.294 \pm 0.011(\text{stat}) \pm 0.008(\text{sys}) \\ &\quad \pm 0.029(\text{lum})\ \text{nb}\end{aligned}$$

DØ assigned a larger uncertainty of 10% on the luminosity. These measurements are in good agreement with expectations.

Similarly $W \to \mu\nu$ and $Z \to \mu\mu$ candidates are easily identified and the products of W and Z production cross sections and their decay branching ratios to muons can be measured. From 7,352 $W \to \mu\nu$ and $1,585 Z \to \mu\mu$ candidates identified from data samples of 17 and 32 pb^{-1} respectively, DØ measured:

$$\begin{aligned}\sigma_W \bullet B(W \to \mu\nu) &= 3.226 \pm 0.128(\text{stat}) \pm 0.100(\text{sys}) \\ &\quad \pm 0.323(\text{lum})\ \text{nb} \\ \sigma_Z \bullet B(Z \to \mu\mu) &= 0.264 \pm 0.007(\text{stat}) \pm 0.017(\text{sys}) \\ &\quad \pm 0.026(\text{lum})\ \text{nb}\,.\end{aligned}$$

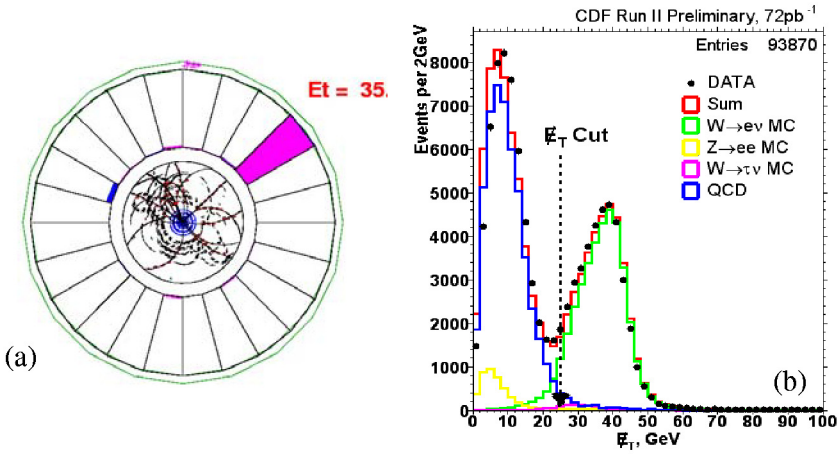

Fig. 7. a End view of a $W \to e\nu$ candidate observed in CDF. The shaded block represents an electron candidate. **b** The distribution of transverse momentum imbalance for events with a high p_T electron

The corresponding CDF measurements are

$$\sigma_W \bullet B(W \to \mu\nu) = 2.64 \pm 0.02(\text{stat}) \pm 0.12(\text{sys}) \pm 0.16(\text{lum})\ \text{nb}$$
$$\sigma_Z \bullet B(Z \to \mu\mu) = 0.246 \pm 0.006(\text{stat}) \pm 0.012(\text{sys}) \pm 0.015(\text{lum})\ \text{nb}$$

Figure 8 compares the Run II measurements at $\sqrt{s} = 1.96$ TeV with those in Run I at $\sqrt{s} = 1.8$ TeV and with theoretical predictions. The uncertainties on the measurements are relatively large, dominated by the errors on luminosity for both CDF and DØ.

Unlike electrons and muons, τ leptons decay soon after their creation, and as such it is difficult to reconstruct and identify them. However, the τ plays important role in searches for Higgs and supersymmetry, mainly due to its large mass. $W \to \tau\nu$ and $Z \to \tau\tau$ decays are ideal final states for studying tau identification. Shown in Fig. 9(a) is an end view of a $Z \to \tau\tau$ candidate event observed in DØ, where one τ decays to muon and neutrinos and the other to three charged pions. Figure 9(b) shows the charge multiplicity distribution of tau candidates identified in CDF. The enhancement in one and three-track bins, expected from single and three-pronged τ decays, are clearly visible. The ability to identify tau leptons at the Tevatron will offer unique physics opportunities. We expect to see many new results based on τ identification in the near future.

3.2 Physics of the top quark

Study of the top-quark production and decay is an important aspect of the Tevatron Run II physics program. Being the last discovered quark, top is the one least understood. Moreover, its large mass, near the scale of electroweak symmetry breaking, suggests that the top quark may be different than the other quarks and leptons. At the Tevatron, most top quarks are pair produced through quark-antiquark annihilation $q\bar{q} \to t\bar{t} + X$. In the standard model, the top quark decays to a b-quark and a W boson with a branching ratio close to 100%. This branching ratio is assumed for most of the studies performed so far. However, both CDF and DØ will be able to test this hypothesis as statistics improves. The final states of $t\bar{t}$ events are often catalogued into the following four categories: 1) dilepton ($ee, \mu\mu, e\mu$) final state, resulting from both Ws decaying to electrons and muons; 2) lepton+jets final state, in which case one W decays to electron or muon while the other decays to hadrons, 3) τ final state, in which one or both Ws decay to τ leptons, and 4) all-jet final state when both Ws decay to hadrons. The dilepton final state is the cleanest channel thanks to the presence of two high pT charged leptons, but suffers from a small branching fraction (∼5%). The lepton+jets channel comes second in small background and has a sizable branching fraction of about 30%. The all-jet channel comprises 44% of all $t\bar{t}$ final states. However, this channel is overwhelmed with multijet background. The τ channel makes up the remaining 21% of the $t\bar{t}$ decays.

The existence of the top quark [9] was established in 1995 by CDF and DØ based on an excess over backgrounds in the dilepton and lepton+jets final states. Since then, convincing signals have also been observed in the all-jet final state [10].

Dilepton candidate events are selected by requiring two high p_T leptons, two jets and large transverse momentum imbalance. The end view of an $e\mu$ candidate event recorded by DØ is shown in Fig. 10(a). From a data sample of 79 pb^{-1}, CDF has observed 1 ee, 1 $\mu\mu$, and 3 $e\mu$ $t\bar{t}$ candidates compared with 0.57±0.08, 0.68±0.09, and 1.5±0.2 events expected from background processes, respectively. The observation yielded a top quark pair production cross section of 13.2±5.9(stat)±1.5(syst) ±0.8(lum) pb. DØ analyzed samples varying from 33 to 48 pb^{-1} for ee, $\mu\mu$, and $e\mu$ signatures, and observed 4 ee, 2 $\mu\mu$, and 1 $e\mu$ candidates with 1.0±0.5, 0.6±0.3, and 0.07±0.01 expected background events, respectively. Assuming the excess is due to $t\bar{t}$ production, it yielded a production cross section of $29.9^{+21.0}_{-15.7}(\text{stat})^{+14.1}_{-6.1}(\text{sys}) \pm 3.0(\text{lum})$ pb.

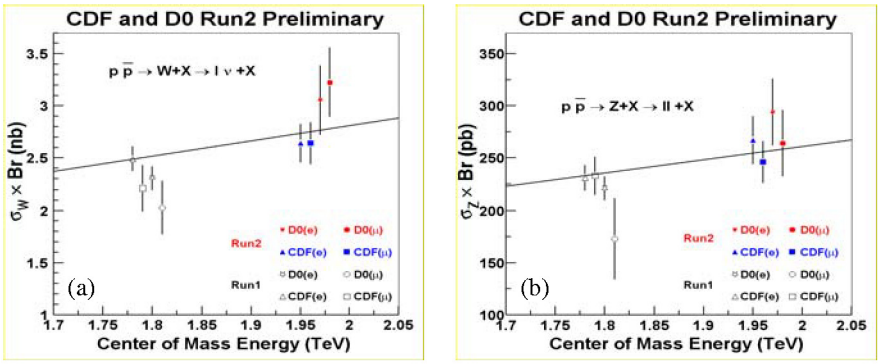

Fig. 8. The $p\bar{p} \to W + X$ production cross section multiplied by the $W \to l\nu$ decay branching ratio obtained at two energies **a**. The $p\bar{p} \to Z + X$ production cross section multiplied by the $Z \to ll$ decay branching ratio. For clarity, the data points are shifted in energy

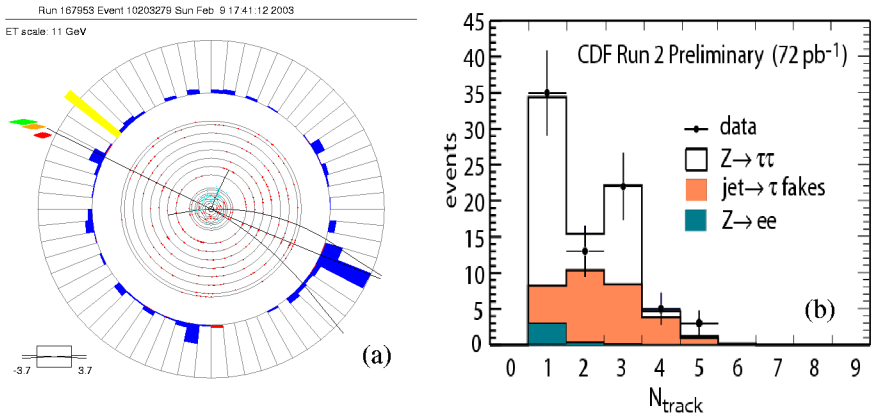

Fig. 9. End view of a $Z \to \tau\tau \to \mu h$ candidate observed in DØ (**a**), and the track multiplicity distribution for CDF τ candidates (**b**)

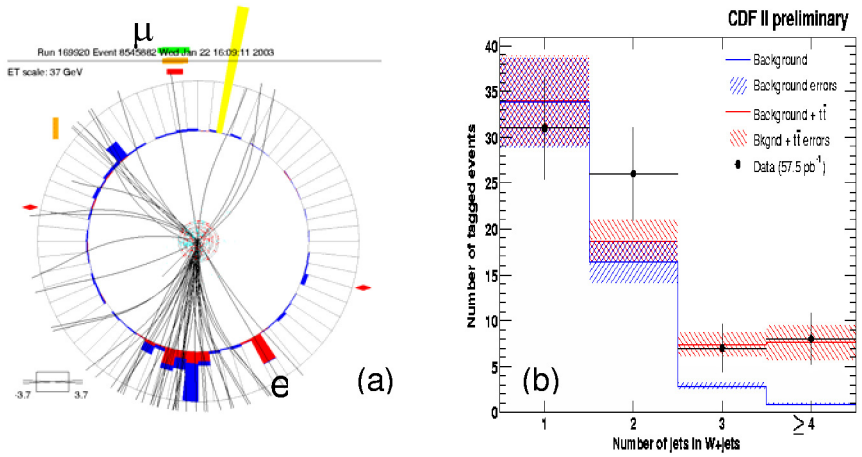

Fig. 10. **a** A DØ $t\bar{t} \to e\mu$+jets candidate, and **b** the CDF jet multiplicity distribution of 1+ jets with at least one b-tagged jet

The lepton+jets events are selected by requiring one high p_T isolated lepton, large transverse momentum imbalance, and multiple jets. CDF required candidates to have three or more jets with at least one of the jets tagged as a b-jet from its long decay lifetime. Figure 10(b) shows the inclusive jet multiplicity distribution of events with a high p_T lepton, large transverse momentum imbalance after imposing b-jet tagging, from a sample of 57.5 pb^{-1}. Excess over backgrounds in 3 and 4 jet bins are evident, as expected from the production of $t\bar{t}$ events. A total of 15 events were observed in the 3 and 4 jet bins while only 3.8 ± 0.5 events were expected from back-

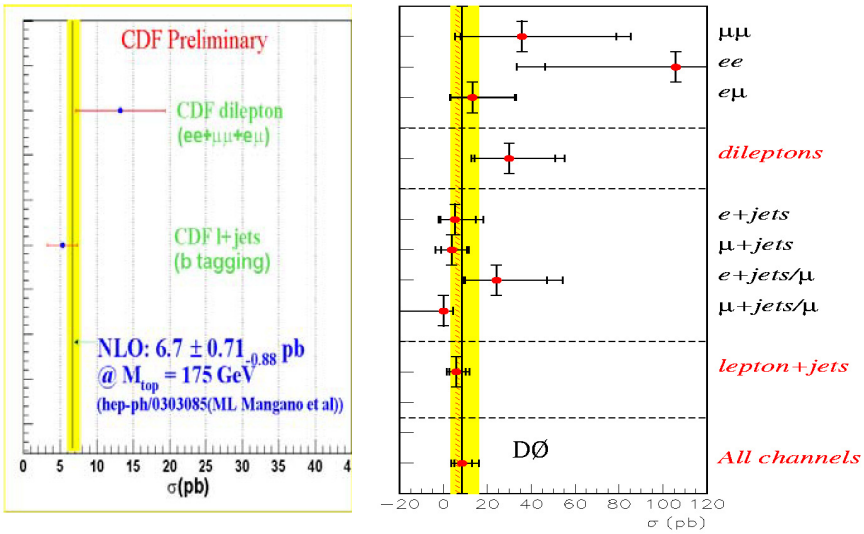

Fig. 11. Summary of CDF and DØ measurements of the $p\bar{p} \to t\bar{t} + X$ cross section in different channels, compared with the theoretical expectation. The gray band represents theoretical uncertainties

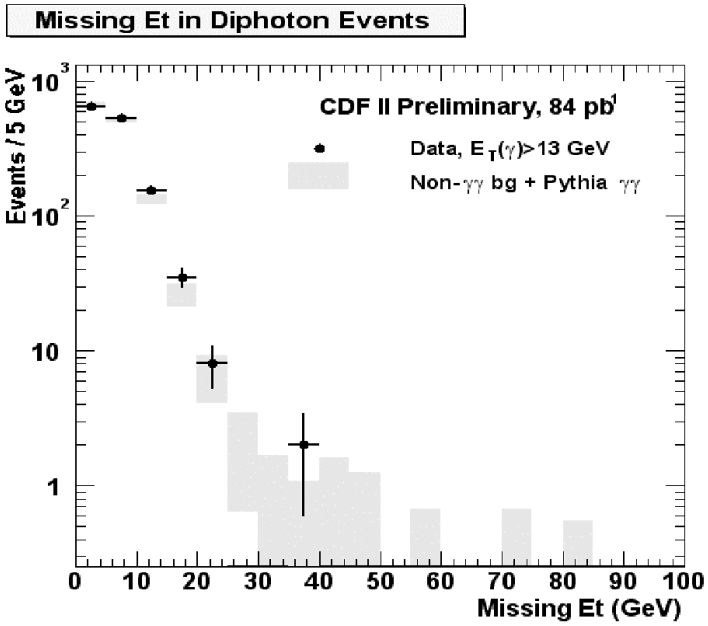

Fig. 12. The distribution of transverse momentum imbalance for diphoton events at CDF compared with that expected from known sources. The two distributions agree well

grounds. The excess led to a cross section of $\sigma_{t\bar{t}} = 5.3 \pm 1.9$ (stat) $\pm$ 0.8(sys) $\pm$ 0.3(lum) pb. DØ pursued two different analyses, one based on event topology and the other on b-jet tagging from b semileptonic decay to a soft muon. In the topological analyses, 8 candidate events were observed with an estimated background of 5.4 ± 1.3. For the soft-muon-tag analysis, 2 candidates were selected with 0.9 ± 0.4 estimated background events. Combining the two methods, DØ measured a cross section of $5.8^{+4.3}_{-3.4}(\text{stat})^{+4.1}_{-2.6}(\text{sys}) \pm 0.6(\text{lum})$ pb at $\sqrt{s} = 1.96$ TeV. These measurements are to be compared with the expected cross section of 6.7 ± 0.7 pb [11] for a 175 GeV top quark. A summary of CDF and DØ measurements is shown in Fig. 11.

CDF also made a preliminary measurement of the top-quark mass from the lepton+jets candidate events. The result is consistent with those obtained in Run I.

3.3 Search for new phenomena

Both CDF and DØ reported a large number of analyses searching for new particles or effects beyond the standard model. Some of the results reported at the symposium already have sensitivities comparable to those of Run I.

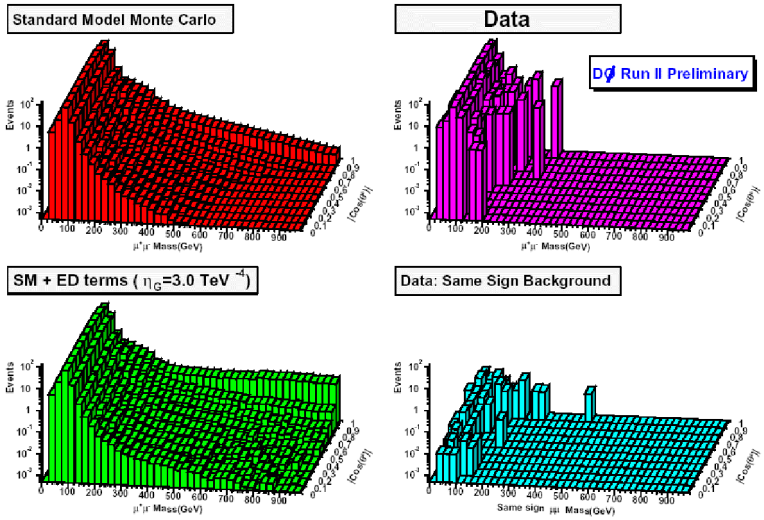

Fig. 13. Two-dimensional distributions of $M_{\mu\mu}$ vs $\cos\theta^*$ expected from the standard model, standard model with large extra-dimensions, background processes compared with that observed in the data

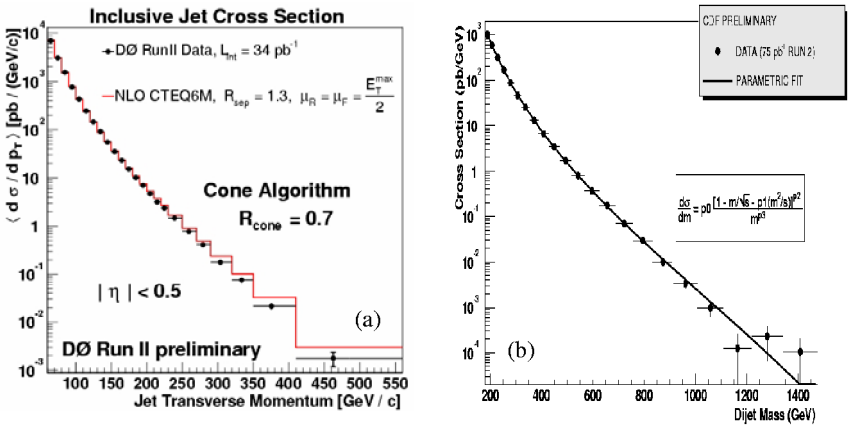

Fig. 14. The differential cross sections for inclusive jet production measured by DØ (**a**) and the dijet invariant mass measured by CDF (**b**)

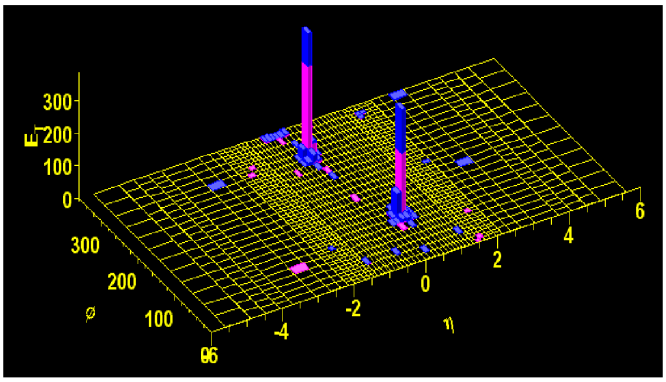

Fig. 15. Lego plot of a high-mass dijet event observed at CDF. The two tall towers represent two high-energy jets produced essentially back-to-back

As examples, I will discuss briefly the searches for diphoton events with large transverse momentum imbalance at CDF, and for large extra dimensions at DØ.

Diphoton events with large missing transverse momentum are expected in many supersymmetry models, such as those involving gauge-mediation. However, experimental

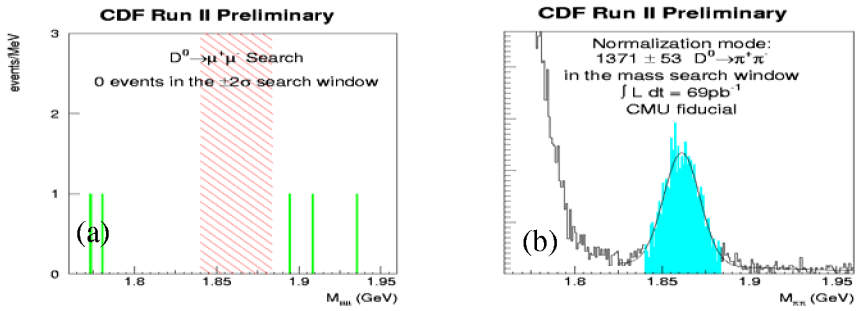

Fig. 16. The variant mass distribution of **a** $\mu^+\mu^-$ and **b** $\pi^+\pi^-$ combinations

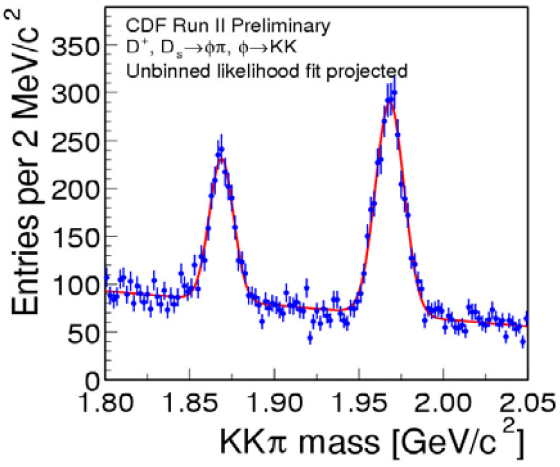

Fig. 17. The invariant mass distribution of $KK\pi$ combination observed at CDF. The $D^{\pm}$, $D_S^{\pm}$ resonances are expected from their decays to $\varphi\pi^{\pm}$, with $\varphi \to K^+K^-$

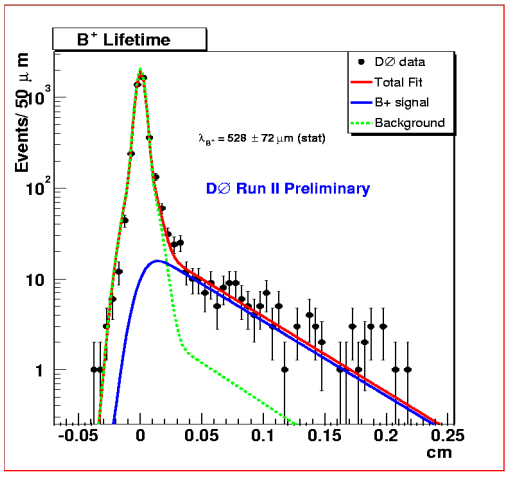

Fig. 18. The distribution of proper decay length for $B^{\pm} \to J/\psi K^{\pm}$ candidates, with overlays from expected signal and background

interest in this class of events is largely motivated by the observation of a rare "$ee\gamma\gamma$" event by CDF in Run I [12]. It is therefore of special interest to search for similar events in Run II. CDF analyzed 84 pb^{-1} of Run II data, looking for diphoton events with photon transverse energies above 13 GeV. Figure 12 shows the observed transverse momentum imbalance distribution of such events compared with that expected from background. The two distributions agree, and there is no outstanding candidate in the sample.

There has been considerable theoretical and experimental interest on the possible existence of large extra-dimensions. Their presence would modify both the mass and angular distributions of dilepton and diphoton events at the Tevatron [13] caused by additional contributions from the exchange of Kaluza-Klein gravitons [14]. Both CDF and DØ have searched for such anomalies. The DØ 2-dimensional distributions in $M_{\mu\mu}$ versus $\cos\theta^*$ expected for purely the standard model, for the SM with large extra-dimensions, just the background events and that observed for the data, are shown in Fig. 13. ($\cos\theta^*$ is the $\mu\mu$ scattering angle in their center-of-mass system.) The existence of large extra dimensions leads to an excess of events at large $M_{\mu\mu}$ and large $|\cos\theta^*|$. No excess is observed. Limits on the effective Planck scale are set using different formalisms.

3.4 Studies of jet production

Jet production is the dominant high p_T process at the Tevatron and therefore one of the major background sources for many other processes of interest. Study of jet production is not only important in its own right, but also for clarifying other high p_T physics. It is fair to say that most of the effort of many analyses of high p_T physics is directed towards understanding backgrounds that often result from jet production.

Both CDF and DØ reported preliminary results on inclusive jet and dijet-mass production cross sections, as shown in Fig. 14. The results are in good agreement with expectations of QCD. The statistical uncertainties on these measurements are generally small, except at very high p_T or high mass regions. However, the systematic uncertainties from the jet energy scale are large due to the sharp drop of the spectra at large p_T.

Figure 15 shows an extremely high-mass dijet event recorded in the CDF detector, with a mass of 1364 GeV, corresponding to about 70% of the $p\bar{p}$ beam energy and a

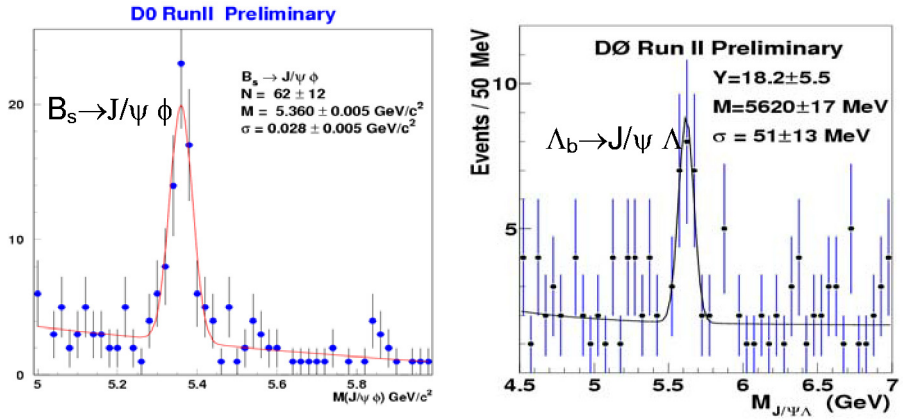

Fig. 19. The invariant mass distributions of **a** $J/\psi\varphi$ and **b** $J/\psi\Lambda$ combinations, where the J/ψ are reconstructed from their decays to $\mu\mu$, and the Λ are identified from their decays to $p\pi$

mean value of 0.85 for the fraction of proton (or antiproton) energy carried by a parton. Of course, events of this kind are expected from rare standard-model processes.

3.5 Beauty and charm physics

The $p\bar{p} \to b\bar{b} + X$ production cross section is ~ 150 μb at $\sqrt{s} = 1.96$ TeV, which implies ~10,000 $b\bar{b}$ events produced every second. This is about 3 orders of magnitude over the rate of PEP-II and KEK-B. However, comparing to the total interaction rate of $\sim$ 2MHz, the b-quark production at the Tevatron is relatively rare. These events are triggered by their decays to muons (CDF and DØ) and their long decay lifetime (CDF). Both experiments presented a variety of preliminary results at this symposium, and more were shown at the recent summer conferences. Much more is yet to come!

I will discuss just two results on charm mesons from CDF: the limit on the branching ratio $B(D^0 \to \mu\mu)$ and mass difference between $D_S^\pm$ and $D^\pm$. These results are made possible by the two-track secondary vertex trigger of CDF. The $D^0 \to \mu^+\mu^-$ decay is strongly suppressed in the standard model. However, the rate can be enhanced dramatically by new physics, as predicted in several models. CDF searched for $D^0 \to \mu^+\mu^-$ decays, and Fig. 16(a) shows the $\mu\mu$ invariant mass distribution from a sample of 69 pb^{-1}. No event is observed in the D^0 mass window. Normalizing this to the observed $D^0 \to \pi^+\pi^-$ decays shown in Fig. 16(b), CDF set a limit of $B(D^0 \to \mu^+\mu^-) < 3.1 \times 10^{-6}$ at 95% C.L. This represents the most stringent limit on the decay mode to date.

CDF also presented a precise measurement of the mass difference between $D^\pm$ and $D_S^\pm$ mesons from their common decays to $KK\pi$:

$$M(D_S^\pm) - M(D^\pm) = 99.28 \pm 0.43(\text{stat}) \pm 0.27(\text{syst})\ \text{MeV/c}^2$$

Figure 17 shows the invariant mass distribution of the $KK\pi$ combination with clear signals for $D^\pm$ and $D_S^\pm$ resonances from a data sample of 5.8 pb^{-1}. The measurement again represents the most precise single measurement, and is the subject of the first Run II physics publication from the Tevatron [15].

The new magnetic tracking system of the upgrade offers many opportunities for studying charm and beauty physics at DØ. The new detector allows DØ to reconstruct resonances and to measure lifetimes of short-lived particles. Though relatively new to this area of physics, DØ presented many preliminary results on B-hadron lifetimes. Shown in Fig. 18 is the distribution of the proper decay length of charged B meson reconstructed from $B^\pm \to J/\psi K^\pm$. A fit yields a lifetime of 1.76 ± 0.24 (stat) ps, consistent with the PDG average of 1.67 ± 0.02 ps. Effort is underway to understand systematics. As another example of what to expect in the near future, Fig. 19 shows the reconstructed B_S and Λ_b mass distributions from a sample of about 40 pb^{-1}. I should point out that CDF and DØ have the word's largest samples of B_S and Λ_b, and I am sure this will provide exciting B physics results over the next few years.

4 Conclusions

The startup of Tevatron Run II has been slow and difficult. The luminosity profile has been revised downwards, the latest conservative plan projects an integrated luminosity of 1.5 fb^{-1} by October 2006 and of 4.4 fb^{-1} by October 2009. However, the new luminosity profile does not change the fact that the Tevatron remains the world's highest energy collider in operation before the LHC turns on. As indicated at this symposium, CDF and DØ have already presented a great deal of interesting physics, and this will continue and expand throughout this decade.

Acknowledgements. I thank the Fermilab beams division for delivering the luminosity, and the CDF and DØ collaborations for their wonderful results that made my presentation possible. In particular, I'd like to express my gratitude to M. Church, T. Ferbel, A. Goshaw, B. Klima, N. Lockyer, R. Moore, J. Spalding, J. Womersley and many others for their assistance

in preparing this talk and proceeding. Finally, I thank the organizers of this symposium for their hard work and for inviting me to present this summary.

References

1. Run II Upgrade Project: `http://www-bd.fnal.gov/run2upgrade`
2. The Run II Luminosity Upgrade at the Fermilab Tevatron: `http://www-bd.fnal.gov/doereview03/docs/Overview7.1.pdf`
3. M. Witherell, Decision on Run II Detector Upgrades: `http://www.fnal.gov/pub/now/Upgrade_Decision/index.html`
4. CDF Collaboration: *The CDF II Detector Technical Design Report*, Fermilab-Pub-96/390-E (1996)
5. DØ Collaboration: *The DØ Upgrade: The Detector and Its Physics*, Fermilab Pub-96/357-E (1996)
6. G. Veramendi: *Recent Results in High pT Physics from CDF*, this proceeding; M. Bishai: *Beauty and Charm Physics at CDF Run II*, this proceeding
7. C. Gerber: *Recent Results and Prospects for High pT Physics at DØ*, this proceeding; G. Borissov: *B-physics at DØ*, this proceeding
8. R. Hamberg, W.L. van Neerven, and T. Matsura: Nucl. Phys. B **359**, 343 (1991); W.L. van Neerven and E.B. Zijlstra: Nucl. Phys. B **382**, 11 (1992)
9. CDF Collaboration, F. Abe et al.: Phys. Rev. Lett. **74**, 2627 (1995); DØ Collaboration, S. Abachi et al.: Phys. Rev. Lett. **74**, 2632 (1995)
10. DØ Collaboration, B. Abbott et al.: Phys. Rev. Lett. **83**, 1908 (1999)
11. E. Gerger and H. Contopanagos: Phys. Rev. D **57**, 253 (1998); R. Bonciani et al.: Nucl. Phys. B **529**, 424 (1998); N. Kidonakis: Phys. Rev. D **64**, 014009 (2001)
12. CDF Collaboration, F. Abe et al.: Phys. Rev. D **59**, 092002 (1999)
13. Th. Kaluza, Sitzsber.: Preuss. Akad. Wiss. Phys. Math. Klasse, 1921, 996 (1921); O. Klein: Z. Phys. **37**, 895 (1926); O. Klein: Nature (London) **118**, 516 (1926)
14. K. Cheung and G. Landsberg: Phys. Rev. D **62**, 076003 (2002)
15. CDF Collaboration, D. Acosta et al.: Fermilab-Pub-03/048-E, submitted to Phys. Rev. D.